Relationship between Macroscopic and Microscopic Models of Surfactant Adsorption Dynamics at Fluid Interfaces

Benedict J. Reynolds,† Megan L. Ruegg,† Nitash P. Balsara,*,†,‡ and C. J. Radke*,†,§

Department of Chemical Engineering, University of California, Berkeley, California 94720, Materials Sciences Division and Environmental Energy Technologies Division, Lawrence Berkeley National Laboratory, University of California, Berkeley, California 94720, and Earth Science Division, Lawrence Berkeley National Laboratory, University of California, Berkeley, California 94720

Received March 2, 2006. In Final Form: July 18, 2006

In a companion preceding paper, we presented an experimental investigation into the adsorption dynamics of a diblock copolymer surfactant to a polymer/polymer interface and found them to be well-described by a microscopic model of diffusion in a potential generated using self-consistent field theory. We compare the predictions of the microscopic approach with a macroscopic (adsorption−diffusion) model and demonstrate the equivalence of the two models when the free-energy well underlying surfactant adsorption is flanked by barriers that are significantly larger than thermal energy (kT). However, when the energy barriers are nonexistent, as is the case for the experimental system of interest, a finite interfacial width must be introduced into the classical model to obtain physically meaningful results (i.e., nonnegative desorption rates). Surprisingly, we find that the predictions of the macroscopic finite interfacial width model with no adjustable parameters are in excellent agreement with experimental data presented in the companion paper even though the latter was obtained with molecular resolution. This agreement provides insight into aspects of the free-energy landscape that determine surfactant transport.

Introduction

This paper is part of a series on the subject of adsorption/desorption of diblock copolymer surfactants at fluid interfaces between two immiscible homopolymers.[1,2] In the first paper, we described measurements of the equilibrium adsorption isotherm of a diblock copolymer at a polymer/polymer interface and successfully compared these measurements with the predictions of self-consistent field theory (SCFT).[2] In the second, companion paper, we described the dynamics of diblock copolymer diffusion through polymer/polymer interfaces in the linear region of the adsorption isotherm (Henry's region).[1] The experimental results were compared with the application of the Smoluchowski equation to a free-energy landcape, $U(z)$, generated using SCFT. In this contribution, we explore the relationship between the field-based (microscopic) approach used in ref 1 and the classical (macroscopic) theories of surfactant transport to understand sorption dynamics at fluid/fluid interfaces.[3−5] We identify which aspects of the free-energy landscape used in the preceding paper were responsible for agreement with the theory.

In classical thermodynamics, interfaces at equilibrium are modeled as infinitesimally thin regions. Extensive thermodynamic properties of the interface such as free energy are conveniently described by surface excess functions. The interfacial excess free energy per unit of interfacial area (i.e., the interfacial tension), γ, and the excess number of surfactant molecules adsorbed per unit of interfacial area, Γ, are two such variables.

At equilibrium, it is straightforward to relate quantitatively the measurable macroscopic properties and continuous interfacial density profiles. The adsorbed amount is the integral of the excess surfactant mole numbers across the interface, while the interfacial tension is the integral of the difference between tangential and normal stresses. This paper is limited to a discussion of Γ. Away from equilibrium, the mapping of dynamic field-based models onto the classical macroscopic description is not entirely straightforward. In classical macroscopic theories, the adsorption/desorption processes are described by pseudo-chemical reactions with rate constants for the conversion of nonadsorbed species to adsorbed species.[3−14] In this limit, surfactant transport is modeled by conventional diffusion, with adsorption and desorption rates appearing as interfacial boundary conditions.

Brenner and Leal[15] addressed the relationship between macroscopic and microscopic interfacial transport by considering the case of constant flux of surfactant molecules across a fluid/fluid interface and arrived at a relationship between the interfacial mass-transfer resistance, R_I; the free-energy field, $U(z)$; and the

* Address correspondence to either author. E-mail: nbalsara@berkeley.edu (N.P.B.) or radke@berkeley.edu (C.J.R.).

† Department of Chemical Engineering, University of California.

‡ Materials Sciences Division and Environmental Energy Technologies Division, Lawrence Berkeley National Laboratory.

§ Earth Science Division, Lawrence Berkeley National Laboratory.

(1) Reynolds, B. J.; Ruegg, M. L.; Mates, T. E.; Radke, C. J.; Balsara, N.P. *Langmuir* **2006**, *22*, 9192−9200.

(2) Reynolds, B. J.; Ruegg, M. L.; Mates, T. E.; Radke, C. J.; Balsara, N. P. *Macromolecules* **2005**, *38*, 3872.

(3) Ward, A. F. H.; Tordai, L. *Nature* **1944**, *154*, 146.

(4) Blair, C. M. *J. Chem. Phys.* **1948**, *16*, 113.

(5) Baret, J. F. *J. Phys. Chem.* **1968**, *72*, 2755.

(6) Baret, J. F.; Bois, A. G.; Casalta, L.; Dupin, J. J.; Firpo, J. L.; Gonella, J.; Melinon, J. P.; Rodeau, J. L. *J. Colloid Interface Sci.* **1975**, *53*, 50.

(7) Diamant, H.; Ariel, G.; Andelman, D. *Colloids Surf. A* **2001**, *183*, 259.

(8) Ferri, J. K.; Stebe, K. J. *Colloids Surf. A* **1999**, *156*, 567.

(9) Ravera, F.; Liggieri, L.; Passerone, A.; Steinchen, A. *J. Colloid Interface Sci.* **1994**, *163*, 309.

(10) Munoz, M. G.; Monroy, F.; Ortega, F.; Rubio, R. G.; Langevin, D. *Langmuir* **2000**, *16*, 1094.

(11) Dukhin, S. S.; Miller, R.; Kretzschmar, G. *Colloid Polym. Sci.* **1983**, *261*, 335.

(12) Svitova, T. F.; Wetherbee, M. J.; Radke, C. J. *J. Colloid Interface Sci.* **2003**, *261*, 170.

(13) Chang, C. H.; Franses, E. I. *Colloids Surf. A* **1995**, *100*, 1.

(14) Lunkenheimer, K.; Serrien, G.; Joos, P. *J. Colloid Interface Sci.* **1990**, *134*, 407.

(15) Brenner, H.; Leal, L. G. *AIChE J.* **1978**, *24*, 246.

10.1021/la060581r CCC: $33.50
Published on Web 09/23/2006

surfactant diffusion coefficient, $D(z)$. They found that this resistance could be positive or negative, depending on the functional form of $U(z)$ in the vicinity of the interface.

Most of the experiments that address surfactant transport to interfaces involve the measurement of dynamic interfacial tension.[6,8,12,14,16−18] In these experiments, the time dependence of the interfacial tension is measured after the surfactant solution is exposed to a suitable interface. Since the equilibrium adsorption data (the measured adsorption isotherm) are known from equilibrium tensiometry, the dynamic interfacial tension data can, in principle, be used to determine the diffusion coefficient of the surfactant and the adsorption/desorption rate constants. There is, however, little agreement between adsorption/desorption rates obtained from different experiments. For example, the measured values of the desorption rate, k_d, for decanol at the air−water interface vary from 10 to 200 s^{-1}.[6,18−20] This disagreement motivated Shin and Abbott to examine the functional form of $U(z)$ using computer simulations.[21] They found that the minimum in $U(z)$ was preceded by a maximum (i.e., a free-energy barrier) on the water side of the water/air interface. The decanol potential energy function is qualitatively different from that for diblock copolymer adsorption at a polymer/polymer interface where no free-energy barrier is present.[1]

In this paper, we study surfactant transport across fluid/fluid interfaces, following the approach of Brenner and Leal.[15] We limit ourselves to the dilute Henry's region of the adsorption isotherm and compare the predictions of macroscopic models with the experimental SIMS data presented in the preceding paper without resorting to any adjustable parameters.

Adsorption−Diffusion Model (Macroscopic)

Consider an interface located between two fluid layers A and B. The dynamics of the surfactant in the bulk phases are described by the diffusion equation

$$\frac{\partial \rho}{\partial t} = D\frac{\partial^2 \rho}{\partial z^2} \quad (D = D_A \text{ in A phase}, D = D_B \text{ in B phase}) \tag{1}$$

and the dynamics of adsorption and desorption affect the interfacial boundary conditions. We consider the adsorption−diffusion model both with and without a finite interfacial width. The case of infinitesimal interfacial width is referred to as the classical adsorption−diffusion model, and the case with a finite interfacial width is referred to as the finite interfacial width adsorption−diffusion model. Let the interfacial region extend from $z = -\lambda_A$ to $z = \lambda_B$, where $z = 0$ is the Gibbs dividing surface. The interfacial boundary conditions then become

$$D_A \frac{\partial \rho}{\partial z}\bigg|_{-\lambda_A} - D_B \frac{\partial \rho}{\partial z}\bigg|_{\lambda_B} = \frac{d\hat{\Gamma}}{dt} \tag{2}$$

and

$$\frac{d\hat{\Gamma}}{dt} = k_{d,A}(\hat{K}_A \rho(-\lambda_A) - \hat{\Gamma}) + k_{d,B}(\hat{K}_B \rho(\lambda_B) - \hat{\Gamma}) \tag{3}$$

In these expressions, z is distance perpendicular to the interface, and $\rho(z)$ is the surfactant number density. For the classical adsorption−diffusion model ($\lambda_A = \lambda_B = 0$), $\rho(-\lambda_A)$ and $\rho(\lambda_B)$ still have distinct values since they correspond to the concentration of surfactant on opposite sides of the infinitesimal interface. D_A and D_B are the diffusion coefficients of the diblock copolymer in the A and B phases, respectively. $\hat{\Gamma}$ is the adsorbed amount in the interfacial region rather than the surface excess, Γ. $\hat{\Gamma}$ therefore includes the "bulk" concentration of the surfactant within the interfacial region. $\hat{\Gamma}$ and Γ are related by

$$\hat{\Gamma} \equiv \Gamma + \lambda_A \rho(-\lambda_A) + \lambda_B \rho(\lambda_B) \tag{4}$$

$k_{d,A}$ and $k_{d,B}$ are the desorption rate constants into the A and B phases, and $\hat{K}_A$ and $\hat{K}_B$ are the equilibrium ratios $\hat{\Gamma}/\rho_A$ and $\hat{\Gamma}/\rho_B$ (Henry's adsorption constants) where ρ_A and ρ_B denote the surfactant densities in the bulk A and B phases. This model assumes that adsorption is in Henry's region of the adsorption isotherm.

Smoluchowski Model (Microscopic)

In the microscopic model, surfactant transport is described by

$$\frac{\partial \rho}{\partial t} = \frac{\partial}{\partial z}\left(D(z)\frac{\partial \rho}{\partial z} - \beta D(z)\frac{dU}{dz}\rho\right) \tag{5}$$

where β is $1/kT$, k is the Boltzmann constant, T is temperature, $U(z)$ is the free-energy field, and $D(z)$ is the diffusion coefficient as a function of position.[22] This model assumes that the surfactant is dilute, that momentum is dissipated on length scales smaller than those over which $U(z)$ changes (the solution is viscous), and that the state of a surfactant molecule can be completely described by its nominal position (i.e., we can average over the other degrees of freedom without affecting the dynamics). These assumptions are not universally valid. Our assumption of dilute surfactant limits discussion to the Henry's region of the adsorption isotherm. The assumption that momentum correlations can be neglected is unreliable for sharp interfaces where the free-energy field experienced by a molecule of surfactant changes abruptly. And finally, the assumption that the state of the surfactant molecule can be completely described by its nominal position, rules out the inclusion of any dynamics of conformational change, which are important for some systems.[10,12] Nevertheless, this model successfully described the experimental results in the companion paper.[1] Details concerning the determination of $\rho(z, t)$ from eq 5 can be found in the companion paper.[1]

Mapping of Equilibrium Behavior

At equilibrium, the criterion to map the two models is that each must predict the same Henry's adsorption constants. The mapping condition thus relates $\hat{K}_A$ and $\hat{K}_B$ from the adsorption−diffusion model to $U(z)$ from the Smoluchowski model. The density profile of surfactant molecules at equilibrium is related to the free-energy field by

$$\rho(z) = Ce^{-\beta U(z)} \tag{6}$$

where C is a constant. Henry's adsorption constant is then given by

$$\hat{K}_A = e^{\beta U_A}\left(\int_{-a}^{b} e^{-\beta U(z)}\,dz - (a - \lambda_A)e^{-\beta U_A} - (b - \lambda_B)e^{-\beta U_B}\right) \tag{7}$$

(16) Phan, C. M.; Nguyen, A. V.; Evans, G. M. *Food Hydrocolloids* **2006**, *20*, 299.
(17) Lin, S. Y.; Tsay, R. Y.; Lin, L. W.; Chen, S. I. *Langmuir* **1996**, *12*, 6530.
(18) Macleod, C. A.; Radke, C. J. *J. Colloid Interface Sci.* **1994**, *166*, 73.
(19) Lin, S. Y.; Lu, T. L.; Hwang, W. B. *Langmuir* **1995**, *11*, 555.
(20) Johnson, D. O.; Stebe, K. J. *J. Colloid Interface Sci.* **1996**, *182*, 526.
(21) Shin, J. Y.; Abbott, N. L. *Langmuir* **2001**, *17*, 8434.
(22) von Smoluchowski, M. *Phys Z* **1916**, *17*, 585.

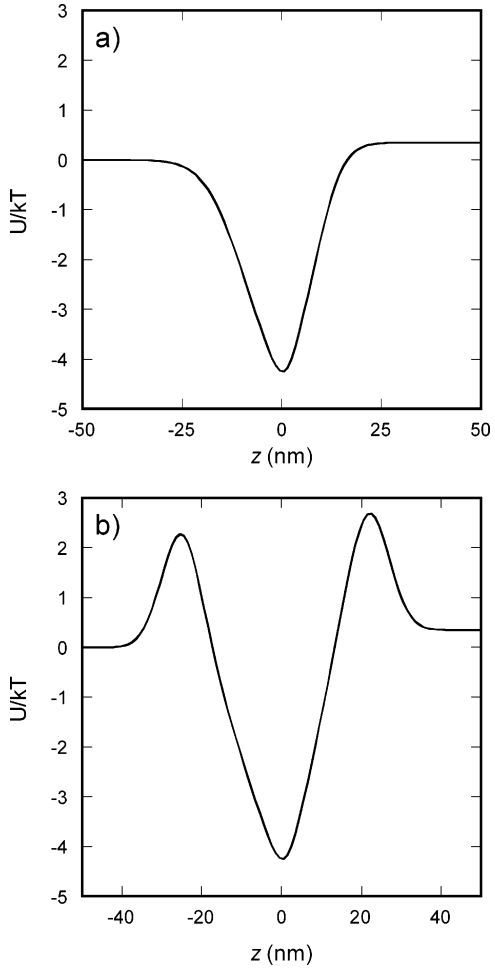

Figure 1. Free energy of a surfactant molecule as a function of ζ for (a) a fluid/fluid interface with no energy barriers to adsorption and (b) a fluid/fluid interface with energy barriers to adsorption.

where $z = 0$ is the Gibbs dividing surface for the fluid/fluid interface, a and b have sufficiently large values such that $z = -a$ and $z = b$ lie outside the interfacial region, and U_A and U_B are the values of $U(z)$ in the bulk A and B phases, respectively. The partition coefficient of the diblock copolymer between the two phases, B, is also found from the free-energy field as

$$B = \frac{\rho_A}{\rho_B} = \frac{\hat{K}_B}{\hat{K}_A} = e^{\beta(U_B - U_A)} \tag{8}$$

and relates the two Henry's constants to one another.

Throughout this work, we use two illustrative energy landscapes (Figure 1a,b) to demonstrate the relationship between the macroscopic and microscopic models. Figure 1a is the SCFT-calculated energy landscape for the experimental system studied in the companion paper.[1] Figure 1b is a similar landscape, but with energy barriers to adsorption added. Applying eqs 7 and 8 to the energy landscape shown in Figure 1a gives $K_A = 699$ nm and $B = 1.41$. Similarly, for the energy landscape shown in Figure 1b, $K_A = 660$ nm and $B = 1.41$.

Mapping of Steady-State Diffusion

Microscopic Model. Following Brenner and Leal,[15] we now consider mapping the classical adsorption−diffusion model to the Smoluchowski model in the case of a constant flux of surfactant across the interface. We perform this mapping for the two qualitatively different energy wells shown in Figure 1. In keeping with the approach of Brenner and Leal, we first characterize these interfaces by examining their mass-transfer resistances. Imagine a surfactant source at $z = -a = -50$ nm, a location that is sufficiently far away from the free-energy well so that diffusion is unaffected by the presence of the well, and a sink at $z = \xi$ with a constant flux, J, between the source and sink. The flux of surfactant molecules can be calculated at any z between $-a$ and ξ from the number density profile $\rho(z)$ and the field in which the molecules diffuse, $U(z)$:

$$J = -D(z)\left(\frac{\partial \rho(z)}{\partial z} + \beta \frac{\partial U(z)}{\partial z}\rho(z)\right) \tag{9}$$

Since J is constant between a and ξ, eq 9 solves directly as

$$J = \frac{\rho(-a) - e^{\beta(U(\xi) - U_A)}\rho(\xi)}{e^{-\beta U_A}\int_{-a}^{\xi} \frac{e^{\beta U(z)}}{D(z)}\mathrm{d}z} \tag{10}$$

A mass-transfer resistance is defined as the driving force divided by the flux. Here there are various possible ways of defining the driving force. Brenner and Leal chose the driving force to be the numerator of eq 10 so that the interval mass-transfer resistance between a and ξ is given by the denominator of eq 10:

$$R(\xi) = e^{-\beta U_A}\int_{-a}^{\xi} \frac{e^{\beta U(z)}}{D(z)}\mathrm{d}z \tag{11}$$

Different acceptable choices of definition for the driving force simply change the resistance by a constant multiplicative factor.

Figure 2a graphs $R(\xi)$, obtained from eq 11 and the energy landscape $U(z)$ shown in Figure 1a. In calculating R, we set the diffusion coefficient, $D(z)$, to 1.08 $\mathrm{nm^2 \cdot s^{-1}}$ for $z < 0$ and to 2.46 $\mathrm{nm^2 \cdot s^{-1}}$ for $z > 0$. These are the measured values of the diffusion coefficient of the diblock copolymer surfactant in the two homopolymers described in ref 1. From Figure 2a, we find that the resistance is a linear function of ξ sufficiently far away from the interface. This is the expected behavior when the mass-transfer resistance in the bulk phase arises due to diffusion alone; the slope $\mathrm{d}R/\mathrm{d}\xi$ is equal to $1/D_A$ in the A phase and B/D_B in the B phase. In the vicinity of the interface, $R(\xi)$ is almost constant (i.e., it does not increase with increasing ξ), implying that there is little mass-transfer resistance at the interface. The physical reason for this result is that the presence of the relatively deep potential well at $z = 0$ means that the concentration of surfactant molecules in this region is much higher than in the bulk. A higher concentration entails higher concentration gradients and, thus, lower mass-transfer resistances. The dotted lines in Figure 2a show the bulk mass-transfer resistances extrapolated to the nominal interfacial position ($z = 0$). From Brenner and Leal, the interfacial mass-transfer resistance, R_I, is defined as excess of the total mass-transfer resistance $R(z = b)$ over that expected by considering the two bulk layers:[15]

$$R_I = R(b) - a\frac{1}{D_A} - b\frac{B}{D_B} = e^{-\beta U_A}\left(\int_{-a}^{0}\left[\frac{e^{\beta U(z)}}{D(z)} - \frac{1}{D_A}\right]\mathrm{d}z + \int_{0}^{b}\left[\frac{e^{\beta U(z)}}{D(z)} - \frac{B}{D_B}\right]\mathrm{d}z\right) \tag{12}$$

where, again, a and b have sufficiently large values that they are outside the interfacial region. The value of R_I for the interface

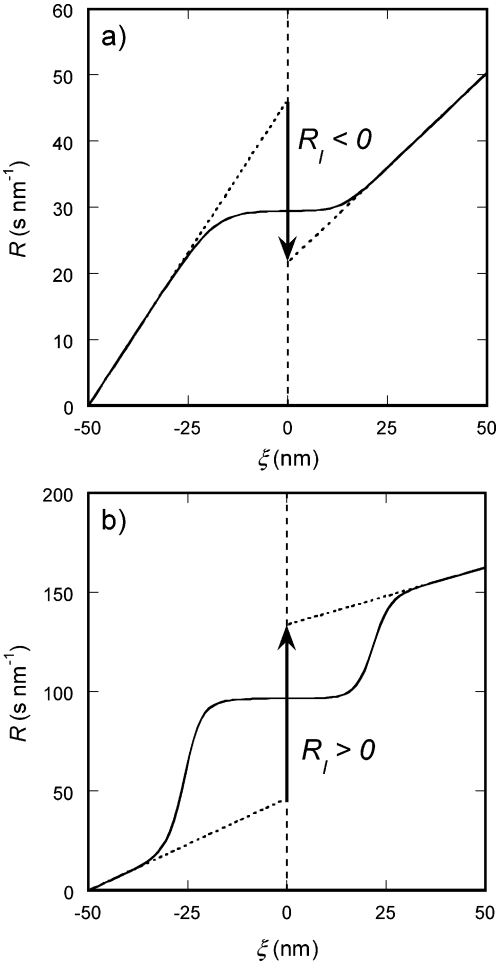

Figure 2. Resistance to mass transfer between points $\zeta = -50$ and $\zeta = \xi$ is plotted against ξ as a solid line for energy landscapes in (a) Figure 1a and (b) Figure 1b. The vertical dashed line indicates the nominal interfacial position, the sloped dotted lines indicate extrapolations of the bulk resistance to the nominal interfacial location, and the bold arrow shows the magnitude of the interfacial mass transfer resistance R_I.

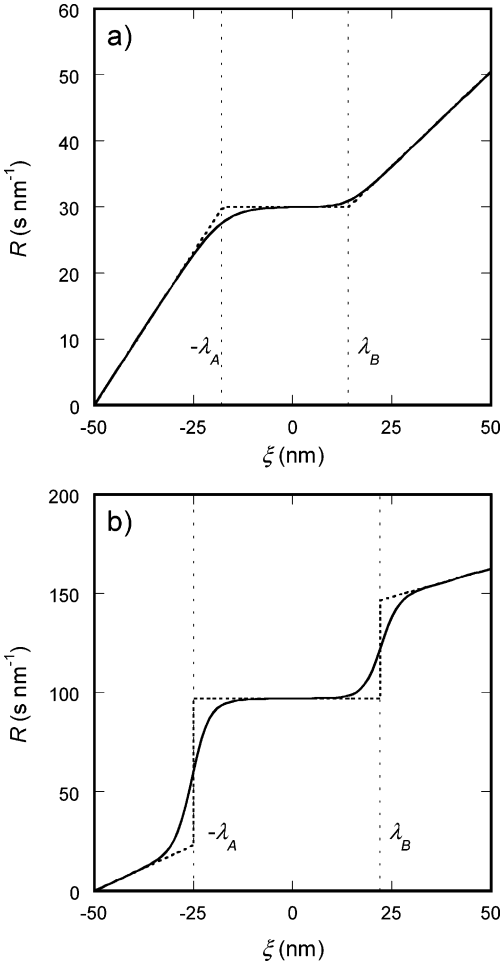

Figure 3. Mass transfer resistance from $\zeta = -50$ nm to $\zeta = \xi$ is plotted against ξ for the free-energy landscapes given in (a) Figure 1a and (b) Figure 1b. The solid line is the results from the Smoluchowski equation, and the dark dotted line is the result of the finite-interfacial width adsorption−diffusion model.

described in Figure 1a is -24 s·nm^{-1} and is represented by the bold arrow in Figure 2a. It is evident from Figure 2a that the finite width of the interface makes a negative contribution to the value of R_I.

Notably, the presence of free-energy barriers has an important affect on the interfacial mass-transfer resistance. In Figure 2b, we graph $R(\xi)$, obtained using eq 11 and the energy landscape $U(z)$ shown in Figure 1b. The same diffusion coefficient profile, $D(z)$, is used to obtain Figure 2a,b. Sufficiently far from the interface (e.g., $|\xi| = 50$ nm), the presence of energy barriers has no effect on $R(\xi)$ (i.e., $R(\xi)$ increases linearly with ξ; Figure 2b). However, $R(\xi)$ increases rapidly in the vicinity of $|\xi| = 25$ nm. This increase in mass-transfer resistance is a manifestation of the free-energy barriers at $z = -25$ nm and $z = 22$ nm in Figure 1b. $R(\xi)$ is nearly independent of ξ in the vicinity of the interface at $\xi = 0$. The interfacial mass-transfer resistance obtained using eq 12 for $U(z)$ from Figure 1b is a positive value, 88 s nm^{-1}, as indicated by the bold arrow in Figure 3b. Note that the introduction of adsorption barriers has changed the sign of R_I.

To permit connection between the macroscopic model where the adsorption−desorption rate constants from the two sides of the interface are treated separately to the microscopic model where the interfacial description is continuous, we decompose the interfacial mass-transfer resistance, R_I, into two resistances on either side of the Gibbs dividing surface, $R_{I,A}$ and $R_{I,B}$. These two quantities are, respectively, as follows:

$$R_{I,A} = e^{-\beta U_A} \int_{-a}^{0} \left[\frac{e^{\beta U(x)}}{D(x)} - \frac{1}{D_A} \right] dx \qquad (13)$$

and

$$R_{I,B} = e^{-\beta U_A} \int_{0}^{b} \left[\frac{e^{\beta U(x)}}{D(x)} - \frac{B}{D_B} \right] dx \qquad (14)$$

Macroscopic Model. We now calculate the mass-transfer resistance through the interface based on the macroscopic adsorption−diffusion model. The flux from $z = -a$ to the subsurface phase at $z = 0$, from the A subsurface phase onto the interface, from the interface to the B subsurface phase, and, finally, from the B subsurface phase to $z = b$ are equal at steady state. Thus, we have that

$$J = D_A \frac{\rho(-a) - \rho(-\lambda_A)}{a - \lambda_A} = k_{d,A}(\hat{K}_A \rho(-\lambda_A) - \hat{\Gamma}) = k_{d,B}(\hat{\Gamma} - \hat{K}_B \rho(\lambda_B)) = D_B \frac{\rho(\lambda_B) - \rho(b)}{b - \lambda_B} \qquad (15)$$

These four equations are solved algebraically for $\rho(-\lambda_A)$, $\rho(\lambda_B)$,

and $\hat{\Gamma}$. The overall mass-transfer resistance between points $z = -a$ and $z = b$ is then given by

$$R = \frac{(a - \lambda_A)}{D_A} + \frac{1}{\hat{K}_A}\left(\frac{1}{k_{d,A}} + \frac{1}{k_{d,B}}\right) + \frac{\hat{K}_B}{\hat{K}_A}\frac{(b - \lambda_B)}{D_B} \quad (16)$$

so that the interfacial mass-transfer resistances are

$$R_{I,A} = \frac{1}{\hat{K}_A k_{d,A}} - \frac{\lambda_A}{D_A} \quad (17)$$

and

$$R_{I,B} = \frac{1}{\hat{K}_A k_{d,B}} - B\frac{\lambda_B}{D_B} \quad (18)$$

By equating the right sides of eqs 13 and 17 and eqs 14 and 18, we obtain a relationship between the parameters in the adsorption−diffusion model ($\hat{K}_A$, B, $k_{d,A}$, $k_{d,B}$, λ_A, and λ_B), and the Smoluchowski model ($U(z)$ and $D(z)$):

$$e^{-\beta U_A}\int_{-a}^{0}\left[\frac{e^{\beta U(x)}}{D(x)} - \frac{1}{D_A}\right]dx = \frac{1}{\hat{K}_A k_{d,A}} - \frac{\lambda_A}{D_A} \quad (19)$$

and

$$e^{-\beta U_A}\int_{0}^{b}\left[\frac{e^{\beta U(x)}}{D(x)} - \frac{B}{D_B}\right]dx = \frac{1}{\hat{K}_A k_{d,B}} - B\frac{\lambda_B}{D_B} \quad (20)$$

The final term in both eqs 19 and 20 disappears for the classical adsorption−diffusion model because $\lambda_A = \lambda_B = 0$. Since $\hat{K}_A$ is known from eq 7 and B is known from eq 8, $k_{d,A}$ and $k_{d,B}$ can be calculated from the free-energy landscape and the diffusion coefficients. For the case of $U(z)$ without free-energy barriers (Figure 1a), there is no possibility of mapping the classical adsorption−diffusion model and the Smoluchowski model because R_I calculated from eq 13 is negative (-24 s·nm^{-1}), whereas the values of $k_{d,A}$ and $k_{d,B}$ must have positive values in order for the model to make physical sense. Even in the limit of infinite adsorption and desorption rate constants, the macroscopic model predicts zero interfacial mass-transfer resistance, which is larger than the negative value given by the microscopic model. Conversely, for the case of $U(z)$ with free-energy barriers (Figure 1b), it is straightforward to show that $k_{d,A} = 3.0 \times 10^{-5}$ s^{-1}, and $k_{d,B} = 4.1 \times 10^{-5}$ s^{-1}. Thus, provided that finite adsorption barriers exist and are large enough so that the interfacial resistance is positive, eqs 19 and 20 enable a direct mapping of the classical adsorption−diffusion model and the Smoluchowski model.

To achieve compatibility between the microscopic and macroscopic models, we remove the restriction that $\lambda_A = \lambda_B = 0$ and consider the finite interfacial width adsorption−diffusion model. The mapping of the Smoluchowski model to the finite width adsorption−diffusion model is best displayed graphically. Figure 2 establishes that the interval mass-transfer resistance, $R(\xi)$, predicted by the Smoluchowski model consists of linear increases in the two bulk phases, almost-horizontal sections in the interfacial region, and sharp nearly vertical jumps where there are energy barriers.

The energy landscape in Figure 1a exhibits no energy barriers to adsorption, and because of this, the interval mass-transfer resistance in Figure 2a shows no sharp increase in the resistance at the edges of the interfacial region. To map the finite interfacial width adsorption−diffusion model to this behavior we set $1/k_{d,A} = 1/k_{d,B} = 0$, so that from eqs 19 and 20, λ_A and λ_B are found to be 18 and 14 nm, respectively.

Table 1. Parameters Used in Mapping the Classical Zero-Width Adsorption−Diffusion Model and Finite InterfacialWidth Adsorption−Diffusion Model to the Smoluchowski Model[a]

	classical adsorption−diffusion model		finite interfacial width adsorption−diffusion model	
	without barriers	with barriers	without barriers	with barriers
$\hat{K}_A$ (nm)	699	660	726	701
B	1.41	1.41	1.41	1.41
λ_A (nm)	0	0	18	25
λ_B (nm)	0	0	14	22
$k_{d,A}$ (s^{-1})	instant[b]	3.0×10^{-5}	instant	1.9×10^{-5}
$k_{d,B}$ (s^{-1})	instant	4.1×10^{-5}	instant	2.9×10^{-5}

[a] All mappings give the correct interfacial mass-transfer resistance except for the classical adsorption−diffusion model with a free-energy landscape without barriers. [b] "Instant" indicates that the surface is assumed to be in equilibrium with the neighboring bulk phase (i.e., infinite desorption rate constant).

In Figure 3a, we compare the interval mass-transfer resistance obtained from the Smoluchowski model (solid curve) with that obtained from the finite interfacial width adsorption−diffusion model using eqs 1−3 (dotted curve) for the potential well of Figure 1a. (The solid curves in Figures 2 and 3 are identical.) It is clear from Figures 2a and 3a that the aphysical negative jump in $R(\xi)$ obtained from the classical zero-width adsorption−diffusion model at the interface (Figure 2a) is eliminated in the finite interfacial width adsorption−diffusion model (Figure 3a).

The interval mass-transfer resistance for the free-energy landscape shown in Figure 1b is plotted in Figure 2b. In this case, $k_{d,A}$ and $k_{d,B}$ have finite values since the resistance increases sharply in the vicinity of the energy barriers. We thus have four independent parameters, $k_{d,A}$, $k_{d,B}$, λ_A, and λ_B, to fit to two equations (19 and 20). We let λ_A and λ_B be the distances from the minimum of the free-energy well to the maximum of the free-energy barriers. This choice, although not unique, makes physical sense because the adsorbed molecules are confined in this region. $k_{d,A}$ and $k_{d,B}$ are then found from eqs 19 and 20.

Figure 3b compares the interval mass-transfer resistance of the Smoluchowski model with the finite interfacial width adsorption−diffusion equation for the potential well in Figure 1b. The proposed mapping procedure captures all features correctly. The interval mass-transfer resistance increases linearly in the two bulk phases, is constant within an interfacial region of width $\lambda_A + \lambda_B$, and makes step increases at the edges of the interfacial region of heights $1/\hat{K}_A k_{d,A}$ and $1/\hat{K}_A k_{d,B}$. It is worth noting that the effective desorption rate constants obtained from adsorption−diffusion models depend on the thickness of the interfacial region.

Parameters obtained using the finite interfacial width adsorption−diffusion model and the classical adsorption−diffusion model for the energy landscapes in Figure 1a,b are summarized in Table 1. In both models, the equilibrium adsorption constant ($\hat{K}_A$ and $\hat{K}_B = B\hat{K}_A$) are higher in the finite interfacial width model than that in the classical model with zero interfacial width. The ratio of equilibrium constants, B, is unaffected by model details as this quantity reflects the properties of the coexisting bulk phases. For the free-energy landscape with barriers, the desorption rates ($k_{d,A}$ and $k_{d,B}$) are substantially smaller in the finite interfacial width model than those in the classical model with zero interfacial width. Differences in the values of the parameters listed in Table 1 highlight the fact that the numerical values of parameters, such as the equilibrium adsorption constants

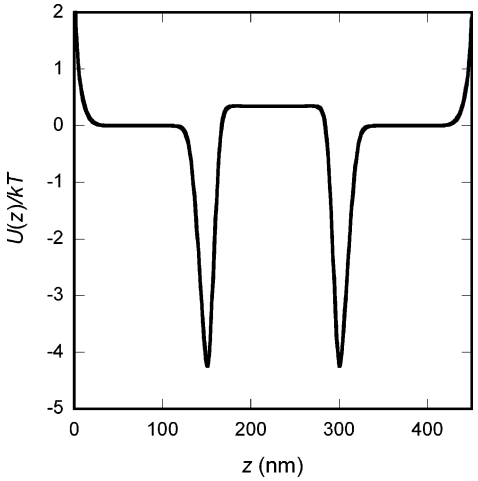

Figure 4. Free-energy landscape calculated by SCFT for the experimental system discussed in ref 1.

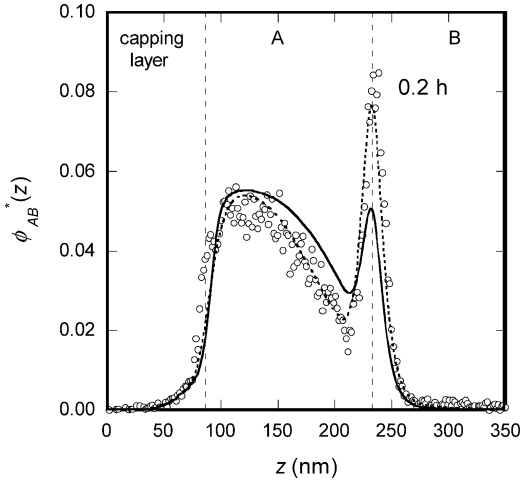

Figure 5. Transient diblock copolymer volume fraction profile as measured by SIMS (open circles) and predicted by the Smoluchowski model (dashed line) and the classical adsorption−diffusion model (solid line).

and the desorption rate constants, are sensitive functions of the model used to interpret the data.

Comparison to Experimental Results

Dynamic Surfactant Concentration Profiles. We now apply the models discussed above to the experimental data presented in the companion paper,[1] where the sorption was measured for a diblock copolymer surfactant to and across an interface between two immiscible homopolymers. The experiment is thoroughly described in ref 1, so we only give a brief description here. Sequential, supported thin polymer films were constructed of a layer of polymer A, followed by a layer of polymer B, and finally by a second layer of polymer A. AB diblock copolymer was initially only present in the upper polymer A layer. Both polymer A layers were 150 nm thick, whereas the polymer B layer was 50, 150, or 600 nm thick. Here we mainly discuss films in which the middle polymer B layer was 150 nm thick. The films were annealed for various amounts of time after which the concentration profile of diblock copolymer surfactant through the film was measured by dynamic secondary-ion mass spectrometry (SIMS).

The location of a diblock copolymer molecule was defined to be that of the junction point between the two blocks. $U(z)$ of a surfactant molecule with its junction point at z, was calculated using SCFT and is shown in Figure 4. In this figure, z ranges from 0 to 450 nm where $z = 0$ and $z = 450$ nm correspond to the interfaces between the A polymer layers and the polystyrene capping layers (PS). The two potential wells in the free-energy landscape correspond to the two A/B polymer/polymer interfaces and are identical to the single potential well shown in Figure 1a. The upturns in $U(z)$ near the two PS/A interfaces show that SCFT predicts that the diblock copolymer is repelled from the two PS/A interfaces. The initial condition for $\rho(z)$ is the equilibrium concentration profile with hard walls at $z = 0$ and $z = 150$ nm. The diffusion coefficients of the diblock copolymer in the A homopolymer and B homopolymer were independently measured to be 1.08×10^{-14} cm^2·s^{-1} and 2.5×10^{-14} cm^2·s^{-1}, respectively.[1] The diffusion coefficient is assumed to change discontinuously at the nominal interfacial positions. With the given free-energy field, $U(z)$, the diffusion coefficient profile, $D(z)$, and the initial condition, $\rho(z, 0)$ prescribed, eq 5 is solved numerically. As demonstrated in our previous work, the resulting microscopic Smoluchowski model using the SCFT-generated potential is in excellent agreement with experimental results for the dynamic diblock copolymer density profiles.[1]

We now apply the adsorption−diffusion model both with and without a finite interfacial width to the same experimental results.[1] Boundary conditions are no-flux at $z = 8$ nm and $z = 442$ nm. The boundaries are moved in from $z = 0$ nm and $z = 450$ nm to account for the repulsion from the PS/A interfaces. The initial condition is that $\rho(z)$ is a constant between $z = 8$ nm and $z = 142$ nm and zero elsewhere. Using the adsorption−diffusion models (eqs 1−3), we calculate $\rho(z, t)$ outside the interfacial regions $\hat{\Gamma}_1(t)$ and $\hat{\Gamma}_2(t)$, the adsorbed amounts at the first and second A/B interfaces, respectively (because we have a trilayer stack, there are two A/B interfaces).

To compare the results of the macroscopic adsorption−diffusion models with the experimental results and with the microscopic Smoluchowski model results, we assume that the transient concentration profile of adsorbed molecules is the same as the equilibrium distribution. With this assumption, $\rho(z, t)$ both outside and inside the interfacial regions is constructed. This number density profile is then converted into a volume fraction profile, $\phi_{AB}^*(z)$, and instrumental smearing effects are taken into account by the methods described in ref 1.

Figure 5 compares the experimental results (open circles) with the predictions of the Smoluchowski model (dashed line) and the classical adsorption−diffusion model with an infinitesimally thin interface (solid line). The classical adsorption−diffusion model uses the parameters in the first column of Table 1. As recorded in our previous paper, agreement between the experimental results and the Smoluchowski model is excellent. However, the classical adsorption−diffusion model fails to capture the adsorption dynamics, predicting that adsorption occurs more slowly than measured experimentally and more slowly than the microscopic Smoluchowski model. Because the classical model neglects the finite interfacial width, it overestimates the distance a surfactant molecule needs to diffuse to reach the interface and thus underestimates the adsorption rate.

Figure 6 is similar to Figure 5, but now for the finite interfacial width adsorption−diffusion model. The open circles and dashed line (hidden behind the solid line) again give the experimental results and the predictions of the Smoluchowski model, respectively; the solid line reflects the finite interfacial width adsorption−diffusion model using the parameters in the third column of Table 1. The finite interfacial width adsorption−diffusion model is in almost exact agreement with the Smoluchowski model and, thus, is also in excellent agreement with the experimental results. This match between experiment, micro-

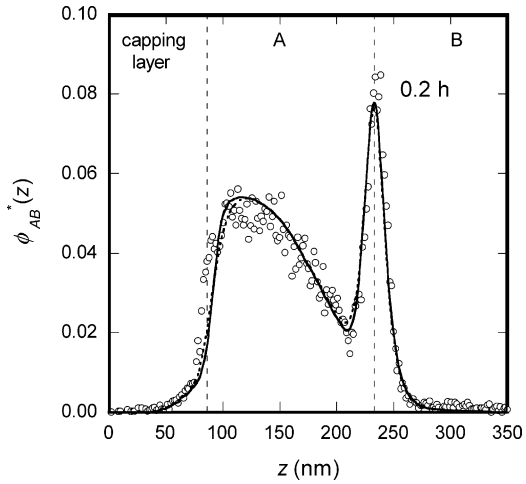

Figure 6. Transient diblock copolymer volume fraction profile as measured by SIMS (open circles), and predicted by the Smoluchowski model (dashed line) and the finite interfacial width adsorption−diffusion model (solid line).

scopic model, and macroscopic model sheds light on what aspects of the free-energy profile, $U(z)$, are responsible for the agreement of the Smoluchowski model with experiment. As long as the free-energy profile correctly predicts the Henry's adsorption constant, $\hat{K}_A$, the partition coefficient, B, and the interfacial width, $\lambda = \lambda_A + \lambda_B$, we expect agreement with experiment to be good. Agreement between the finite interfacial width adsorption−diffusion model and experiment is seen at all of the experimental conditions studied in ref 1.

Clearly, finite interfacial width is necessary to explain our transient experimental results. In general, hindrance to mass-transfer over an interface includes positive resistances in the surrounding bulk phases, a negative contribution from the finite interfacial width, and a positive contribution from the desorption rates (eq 13). The finite interfacial width effect is negligible when the contribution to the resistance from desorption kinetics dominates, $1/\hat{K}_A k_{d,A} \gg \lambda_A/D_A$, or when the length scale (or time scale) probed experimentally is much larger than the interfacial width (or time taken to diffuse across the interfacial width), $a/D_A \gg \lambda_A/D_A$. In our polymeric experimental system, the desorption rate constant is infinite, and our depth resolution is smaller than the interfacial width so we are able to detect the effect of the finite interfacial width on the adsorption rate. Detecting such an effect on a system of small surfactant molecules is difficult since the interfacial widths are much narrower. For typical surfactants, desorption rate constants are large enough that the effect of the finite interfacial width can be neglected. For example, for decanol at the air/water interface $1/\hat{K}_A k_{d,A} \approx 100$ s·m^{-1} and $\lambda/D \approx 1$ s·m^{-1}.[18,21] This is not to say that interfacial width effects are never important for small molecule systems. With strongly adsorbing surfactants, $\hat{K}_A$ is very large and, thus, the effect of the desorption rate is negligible. If two interfaces containing such a strong surfactant are extremely close together, the rate of equilibration of the surfactant between the two interfaces depends on the interfacial width. This effect could be important in microemulsions or in biological systems.

Conclusions

In the companion article,[1] we experimentally measured the adsorption of a diblock copolymer to a polymer/polymer interface and found that the dynamics could be well-described by applying the Smoluchowski equation. We present a methodology for mapping the microscopic Smoluchowski model onto a macroscopic adsorption−diffusion model of surfactant transport across interfaces. The Smoluchowski and adsorption−diffusion models each have advantages and disadvantages. The Smoluchowski model is perhaps more satisfying because, in accordance with the physical system, the interface is seamlessly integrated with the bulk phases. In contrast, the adsorption−diffusion model requires conceptual partitioning of the system into interfacial zones that separate bulk phases. The advantage of the adsorption−diffusion model is that it enables prediction of surfactant transport as long as a few constants, namely, $\hat{K}$, B, D, λ, and k_d are known.

We find that for a free-energy profile with no energy barriers to adsorption (which is the case for the experimental system of interest) it is impossible to map the Smoluchowski model onto an adsorption−diffusion model without taking into account the finite width of the interface. Once this finite width was included into the adsorption−diffusion model, its predictions were almost indistinguishable from those of the Smoluchowski model. That the standard adsorption−diffusion model breaks down near the length scale of the interfacial width comes as no surprise. The surprising and useful result is that a simple inclusion of finite width into the adsorption−diffusion macroscopic model permits quantitative agreement with experimental results even down to the length scale of the interfacial width.

Acknowledgment. This material is based upon work supported by the National Science Foundation under Grant 0305711.

LA060581R